Electronic Supplementary Material (ESI) for Journal of Materials Chemistry A.
This journal is © The Royal Society of Chemistry 2014

Supporting information

A Robust Hydrogen Evolution Catalyst Based on Crystalline Nickel Phosphide Nanoflakes on Three-Dimensional Graphene/Nickel Foam: Ultrahigh Activity for Electrocatalytic Hydrogen Production from pH 0-14

Ali Han, Song Jin, Huanlin Chen, Hengxing Ji, Zijun Sun, Pingwu Du*

CAS Key Laboratory of Materials for Energy Conversion, Department of Materials Science and Engineering, and the Collaborative Innovation Center of Chemistry for Energy Materials (*i*ChEM), University of Science and Technology of China (USTC), Hefei, China 230026

*email: dupingwu@ustc.edu.cn

Experimental Methods

Materials. All chemicals, including nickel foam, red phosphorus, sulfuric acid (H_2SO_4), potassium dihydrogen phosphate (KH_2PO_4), dipotassium hydrogen phosphate (K_2HPO_4), and potassium hydroxide (KOH), were purchased from Aldrich or Acros and used without further purification. Potassium phosphate buffer (1.0 M KPi) were prepared by mixing appropriate dipotassium hydrogen phosphate trihydrate (K_2HPO_4), potassium dihydrogen phosphate (KH_2PO_4) and deionized water. 0.5 M H_2SO_4 solution was prepared by diluting the concentrated sulfuric acid. 1 M KOH solution was prepared by potassium hydroxide and deionized water and the final pH was ~14. All electrolyte solutions were prepared using millipore water (resistivity: ~18 MΩ·cm).

Electrochemical methods.

The electrochemical tests were operated in a home-made three electrode electrochemical cell. All electrochemical experiments were performed at room temperature under air with a 660D CH Instrument potentiostat (purchased from Shanghai Chen Hua Instrument Co., Ltd.). An Ag/AgCl electrode (3 M KCl, the potential is 0.21 V vs. NHE) was used as the reference electrode, Pt wire as the counter electrode and graphene layers (G), G@NF, Ni_2P@G, and Ni_2P-G@NF as the working electrodes. 0.5 M H_2SO_4, 1.0 M KPi and 1 M KOH were used as electrolytes except as otherwise noted. There was several iR drop for compensation and no stirring were used for the polarization curve. Electrocatalysis for measuring Faraday efficiency was carried out with an overpotential of 277 mV by using a sealed electrochemical cell. The reference electrode was placed a few millimeters from the working electrode surface. All potentials reported in this manuscript were converted to the RHE.[1]

Synthesis of 3D Ni_2P networks

Commercial nickel foam (1 × 5 cm) was used as the template and the hybridizing graphene layers/nickel foam (G@NF) was fabricated *via* a simple heating method.[2] Subsequently, a certain amount of red phosphorus powder was evenly sprinkled on the surface of the G@NF. The G@NF was placed in a quartz tube, heated to 750 °C in flowing argon for 1 hour (10 °C/min), and then cooled down to room temperature to obtain the 3 D Ni_2P-G@NF electrode. 3D Ni_2P -G@NF electrode was directly used for the electrochemical activities in 0.5 M H_2SO_4, 1.0 M Pi and 1 M KOH solutions.

To prepare Ni_2P@G electrode without nickel substrate, the Ni_2P-G@NF electrode was put into a 10 mL HCl solution (6 M) and heated to 80 °C for 5 h to remove Ni. Finally, the as-obtained 3D Ni_2P@G was washed with deionized water until it is neutral. Then the G@NF electrode was used to study the electrocatalytic properties in 0.5 M H_2SO_4.

Characterization of 3D Ni_2P networks

Powder X-ray diffraction (XRD). The Ni_2P@G, NF, G@NF and Ni_2P-G@NF electrodes were examined by powder X-ray diffraction (XRD, D/max-TTR III) using graphite monochromatized Cu Kα radiation ($\lambda = 1.54178$ Å), operating at 40 kV and 200 mA. The scanning rate was 5° min^{-1} from 20° to 80° in 2θ.

X-ray Photoelectron Spectroscopy (XPS). The element valence states of the Ni_2P -G@NF was probed with the ESCALAB 250 X-ray photoelectron spectroscopy (XPS).

The survey scan and the high resolution spectra of Ni 2p and P 2p were shown in Figure S4. The spectra are referenced to C1s peak (285.0 eV).

Scanning Electron Microscopy (SEM) and energy dispersive X-ray spectroscopy (EDX). The morphologies of the NF, G@NF, Ni_2P@G and the Ni_2P-G@NF electrodes were examined using a JSM-6700F field emission scanning electron microscope (FE-SEM). The materials were analyzed in several local spots to ensure their chemical homogeneity. The samples were rinsed with deionized water and acetonitrile, and dried in air. Then Au was coated on the surface to make the samples conducting before loading into the instrument. Images were obtained with an acceleration voltage of 5 kV.

Reference

1. Cobo, S.; Heidkamp, J.; Jacques, P. A.; Fize, J.; Fourmond, V.; Guetaz, L.; Jousselme, B.; Ivanova, V.; Dau, H.; Palacin, S.; Fontecave, M.; Artero, V. A Janus Cobalt-based Catalytic Material for Electro-Splitting of Water. *Nat. Mater.* **2012**, 11, 802-807.
2. Ji, H.; Zhang, L.; Pettes, M. T.; Li, H.; Chen, S.; Shi, L.; Piner, R.; Ruoff, R. S. *Nano Lett.* **2012**, *12*, 2446-2451.

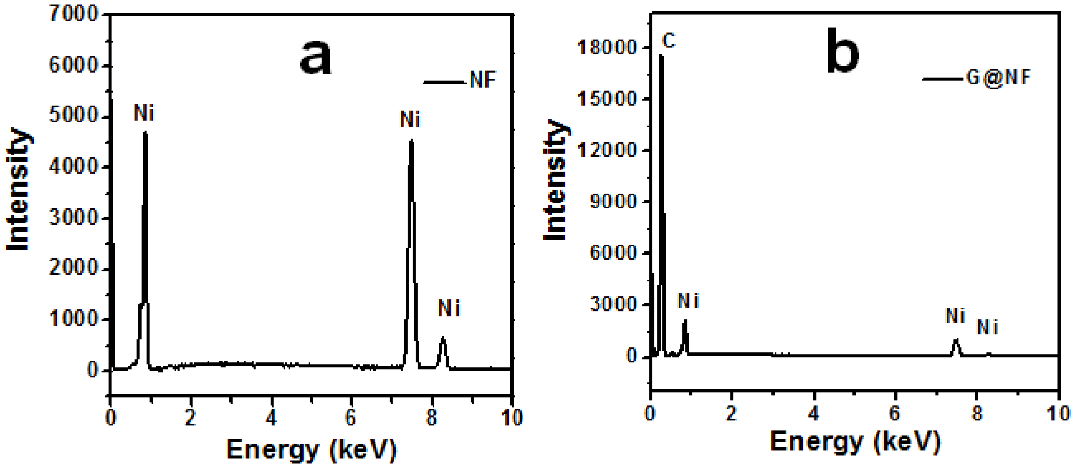

Figure S1. The EDX spectra for the nickel foam (NF, a) and the graphene layers hybridizing nickel foam (G@NF, b).

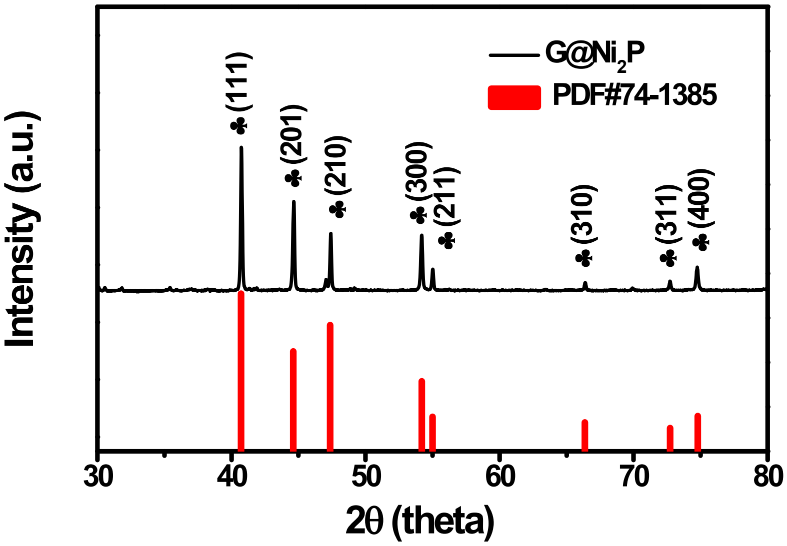

Figure S2. X-ray diffraction patterns of the as-prepared 3D Ni_2P@G (black) and the PDF#74-1385 (red).

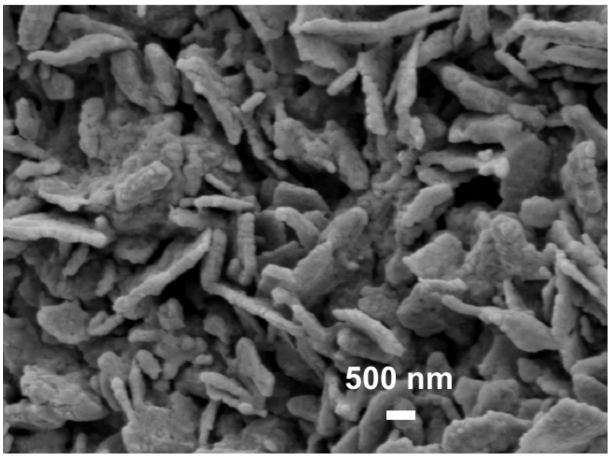

Figure S3. The high magnification SEM image of the Ni_2P nanoflakes.

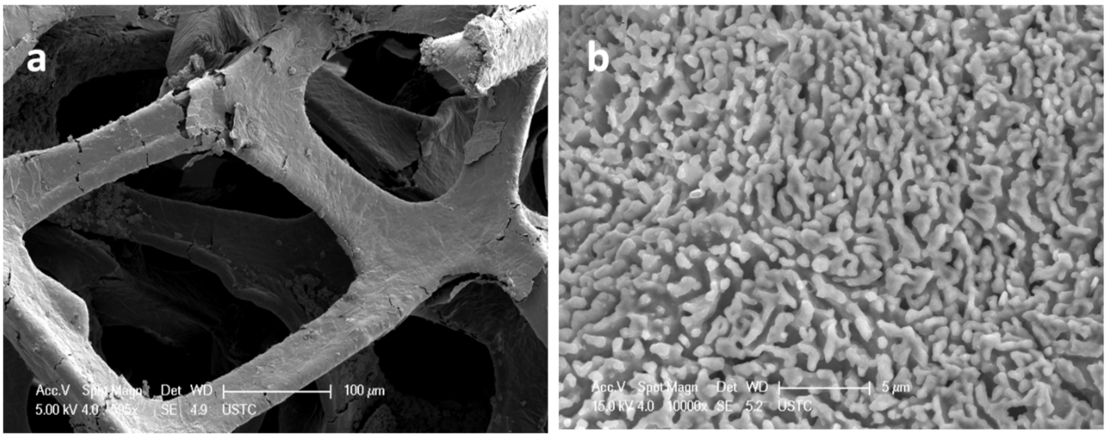

Figure S4. The SEM images for the Ni_2P@G. The nickel substrate is removed in strong acid.

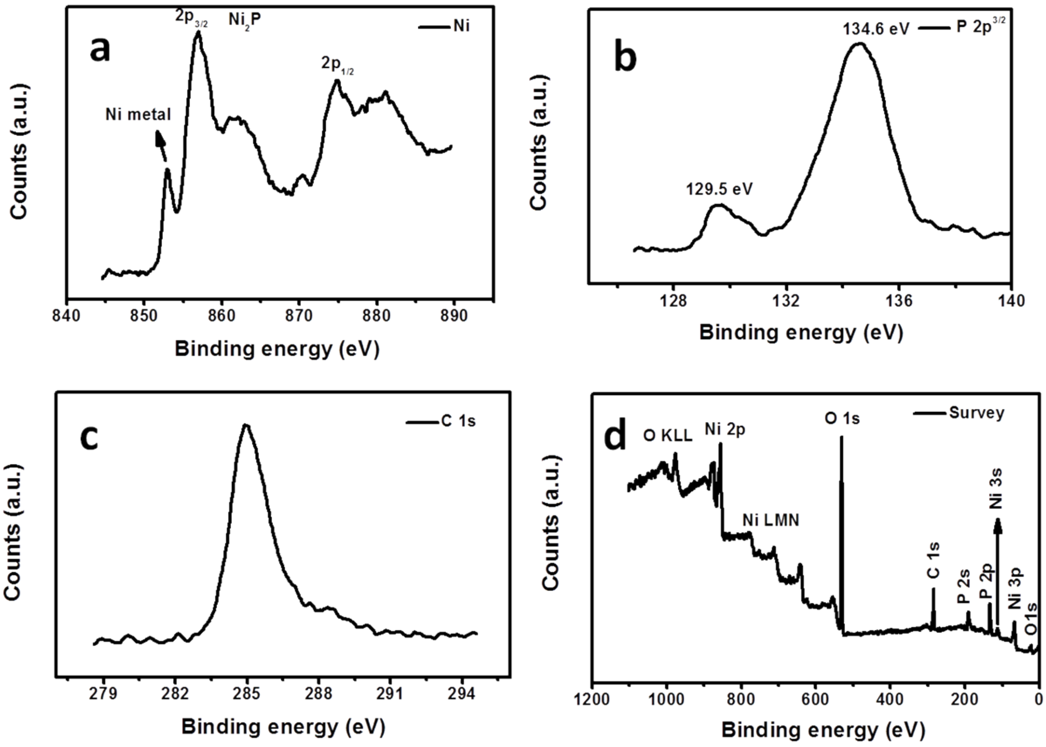

Figure S5. The XPS spectra of (a) Ni 2p, (b) P $2p_{3/2}$, (c) C 1s and (d) the survey spectrum of the as-prepared 3D Ni_2P-G@NF electrode.

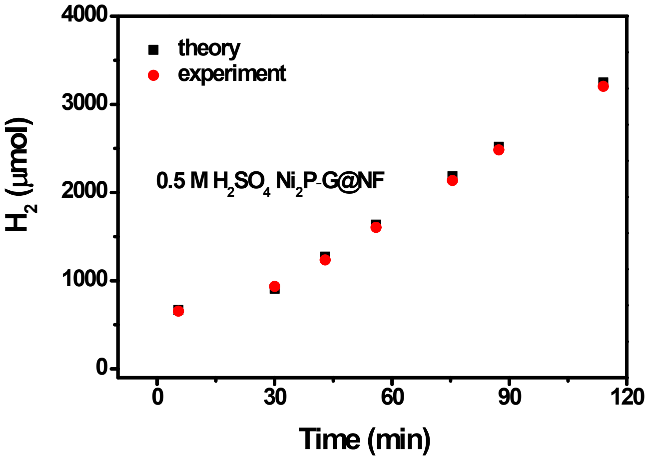

Figure S6. The theoretical (black dot) and experimentally observed (red dot) H_2 production as the function of time in 0.5 M H_2SO_4 solution with Ni_2P-G@NF as the cathode.

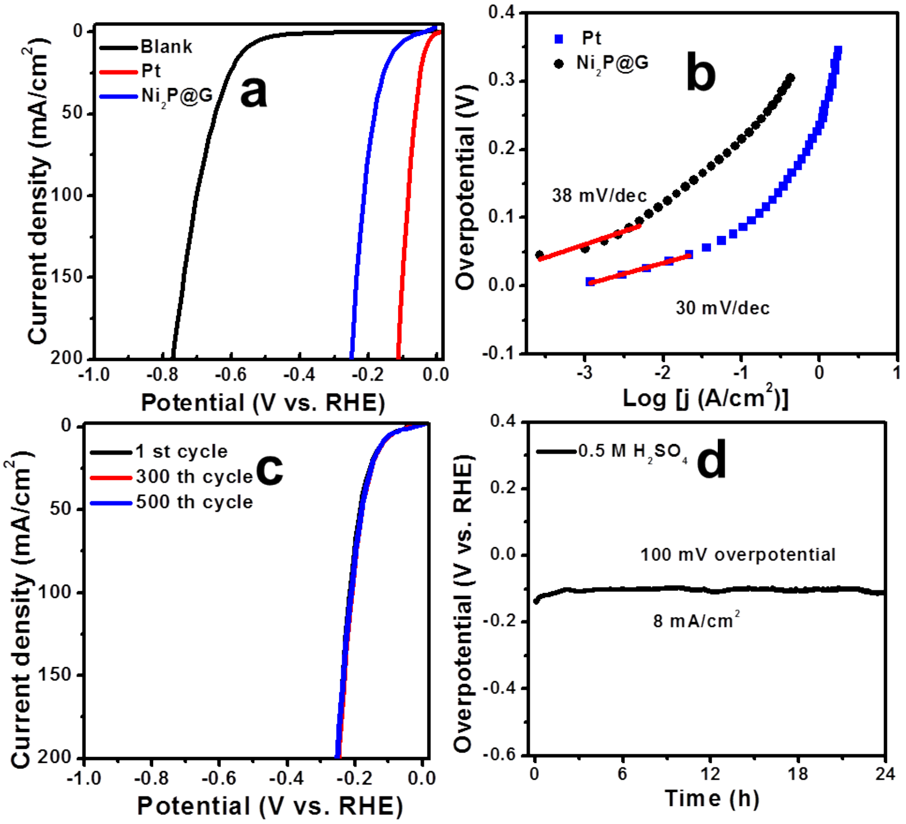

Figure S7. a) Polarization curves of Ni_2P@G electrode in 0.5 M H_2SO_4 (pH ~0) with a scan rate of 5 mV s^{-1}, along with graphene layers and a Pt electrode for comparison. The iR drop was corrected with ~2 Ώ; b) The Tafel plots for the Ni_2P@G electrode and the Pt electrode obtained from the polarization; c) Polarization data for the Ni_2P@G electrode in 0.5 M H_2SO_4 initially and after 300, 500 CV sweeps from 0.10 to -0.30 V vs. RHE; d) Time-dependent current density for Ni_2P@G electrode under an overpotential of 100 mV for 24 h.

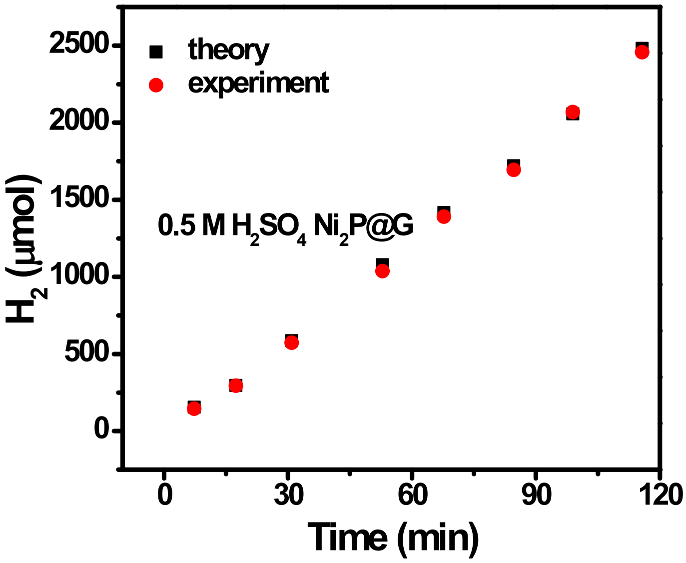

Figure S8. The theoretical (black dot) and experimentally observed (red dot) H_2 production as the function of time in 0.5 M H_2SO_4 solution with Ni_2P@G as the cathode.

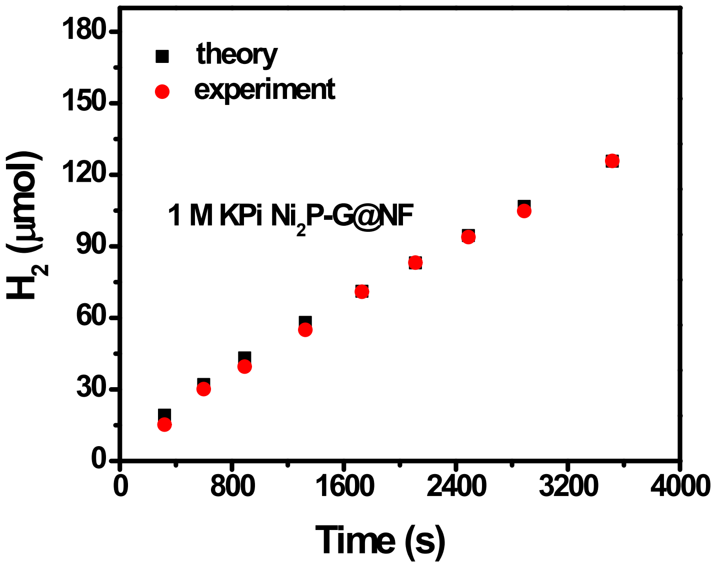

Figure S9. The theoretical (black dot) and experimentally observed (red dot) H_2 production as the function of time in 1 M KPi solution with Ni_2P-G@NF as the cathode.

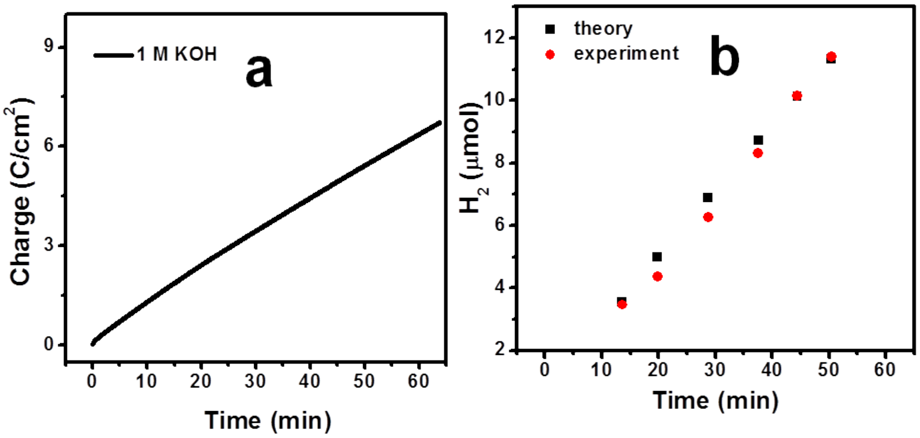

Figure S10. a) The charges during bulk electrolysis, which increased with time under an overpotential of 7 mV in 1.0 M KOH solution; b) The theoretical (black dot) and experimentally observed (red dot) H_2 production as the function of time in 1.0 M KOH solution with Ni_2P-G@NF as the cathode.

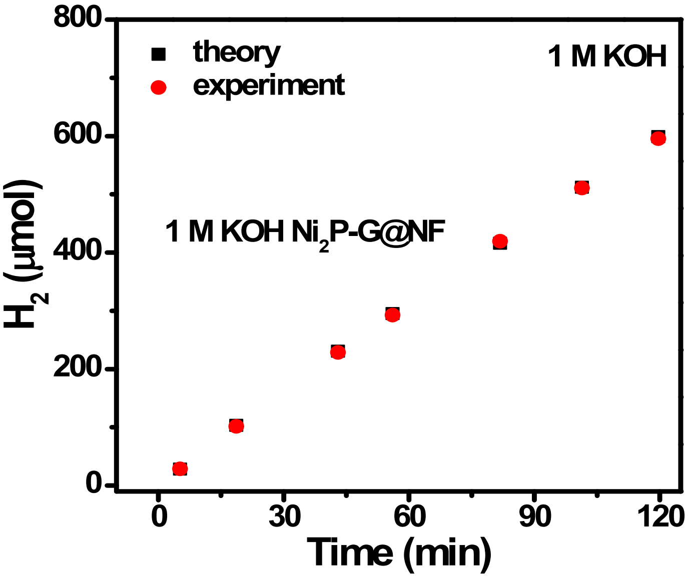

Figure S11. The theoretical (black dot) and experimentally observed (red dot) H_2 production as the function of time in 1 M KOH solution with Ni_2P-G@NF as the cathode.

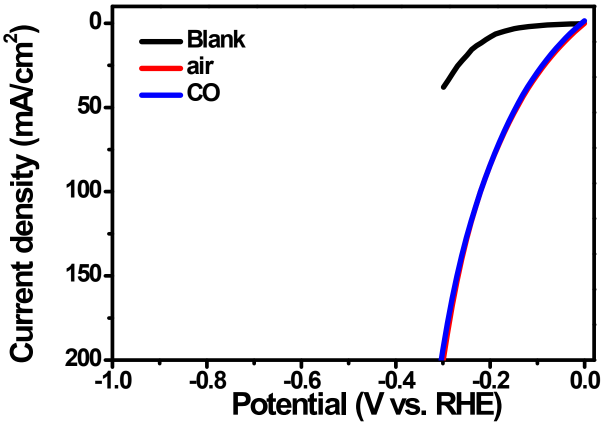

Figure S12. Polarization curves of the Ni_2P-G@NF electrode in 1 M KOH (pH ~14) with a scan rate of 5 mV s^{-1}. Black plot- the G@NF electrode for comparison; red plot - in the presence of air, blue plot - in the presence of CO.

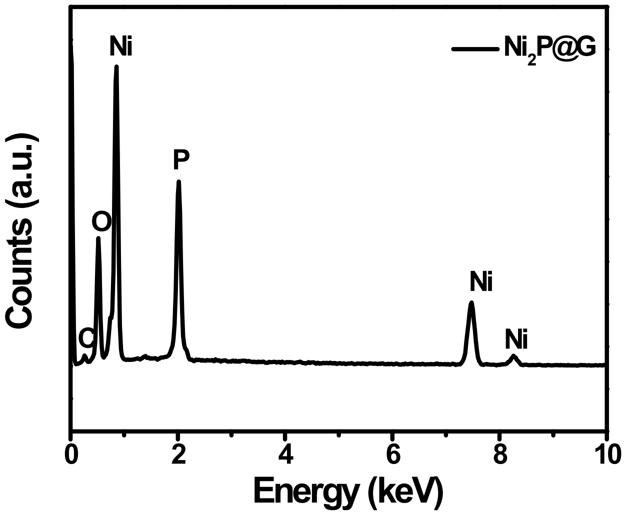

Figure S13. EDX spectrum of the as-prepared 3D Ni_2P@G networks. The atomic ratio of the Ni and P was close to 2:1.

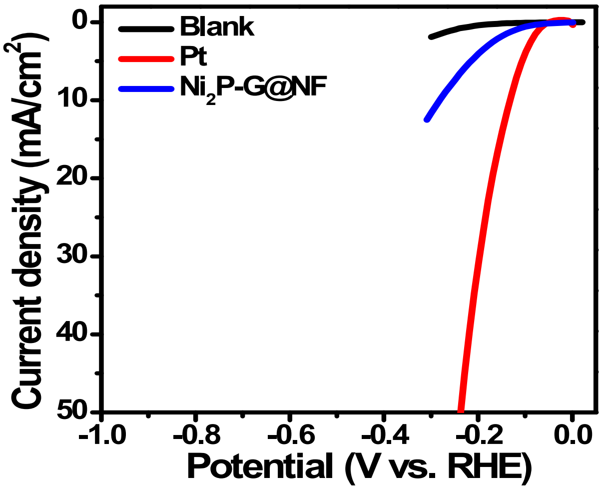

Figure S14. Polarization curves of Ni_2P-G@NF electrode in 1 M KOH (pH ~14) with a scan rate of 5 mV s^{-1}, along with the G@NF electrode and Pt electrode for comparison. Note: the area of the 3D Ni_2P-G@NF electrode and G@NF electrode was normalized to a flat area divided by 20.

Table S1. Comparison of various solid-state HER catalysts in acid solutions.

catalyst	pH	Onset η (mV)	Tafel slope (mV/dec)	Current density (j, mA/cm^2)	η at the corresponding j (mV)	Faraday efficiency	Ref
Ni_2P@G	0	50	38	10	105	~100%	This work
Ni_2P -G@NF	0	30	30	10	55	~100%	This work
CoP/CC	0	38	51	10	67	~100%	*J. Am. Chem. Soc.* **2014**, *136*, 7587.
Pt	0	0	30	2	5	-	*J. Am. Chem. Soc.* **2013**, *135*, 9267.
Ni_2P nanoparticles	0	-	46	10	116	~100%	*J. Am. Chem. Soc.* **2013**, *135*, 9267.
FeP nanosheets	0	100	67	10	~240	-	*Chem. Commun.* **2013**, *49*, 6656.
Fe-MoS_3 film	0	-	39	-	-	-	*Chem. Sci.* **2012**, *3*, 2515.
Co-MoS_3 film	0	-	43	-		-	*Chem. Sci.* **2012**, *3*, 2515.
Ni-MoS_3 film	0	-	42	-		-	*Chem. Sci.* **2012**, *3*, 2515.
Cu-MoS_3 film	0	-	40	-	-	-	*Chem. Sci.* **2012**, *3*, 2515.
Zn-MoS_3 film	0	-	39	-	-	-	*Chem. Sci.* **2012**, *3*, 2515.
MetallicMoS_2 nanosheets	0	200	54	10	195	-	*J. Am. Chem. Soc.* **2013**, *135*, 10274.
MoS_2 particles	0	100	54	2	190	-	*Energy Environ. Sci.* **2012**, *5*, 6136.
MoS_3 film	0	-	39	-	-	-	*Chem. Sci.* **2011**, *2*, 1262.
Nanoporous Mo_2C nanowire	0	70	53	60	200	-	*Energy Environ. Sci.* **2014**, *7*, 387.
Bulk Mo_2C	0	-	87.6	10	240		*Energy Environ. Sci.* **2013**, *6*, 943.
Double-gyroid MoS_2/FTO	0	150-200	50	2	190		*Nat. Mater.* **2012**, *11*, 963.

$CoSe_2$NP/CP	0	-	42.1	10	139	-	*J. Am. Chem. Soc.* **2014**, *136*, 4897.
$CoSe_2$ nanobelts	0	50	48	-	-	-	*Angew. Chem. Int. Ed.* **2013**, *52*, 8546.
Defect-rich MoS_2	0	120	50	13	200	-	*Adv. Mater.* **2013**, *25*, 5807.
MoO_3-MoS_2/FTO	0	150-200	50-60	10	310		*Nano Lett.* **2011**, *11*, 4168.
WS_2 nanosheets	0	80-100	60	-	-	-	*Nat. Mater.* **2013**, *12*, 850.
WS_2/rGO	0	150-200	58	23	300		*Angew. Chem. Int. Ed.* **2013**, *52*, 13751.
MoN/C	1	157	54.5	2	290	-	*Angew. Chem. Int. Ed.* **2012**, *51*, 6131.
$NiMoN_X$/C	1	78	35.9	2	170	-	*Angew. Chem. Int. Ed.* **2012**, *51*, 6131.
Pt/C	1	0	30	2	60	-	*Angew. Chem. Int. Ed.* **2012**, *51*, 6131.

Table S2. Comparison of various solid-state HER catalysts in neutral solutions.

catalyst	pH	Onset η (mV)	Tafel slope (mV/dec)	Current density (j, mA/cm^2)	η at the corresponding j (mV)	Faraday efficiency	Refs.
Ni_2P -G@NF	7	~15	40	2	40	~100%	This work
CoP/CC	7	45	93	2	65	~100%	*J. Am. Chem. Soc.* **2014**, *136*, 7587.
H_2-CoCat film	7	50	140	2	385	-	*Nat. Mater.* **2012**, *11*, 802.
CoS/FTO	7	43	93	2	83	~100%	*J. Am. Chem. Soc.* **2013**, *135*, 17699.
Fe-MoS_3 film	7	-	95	-	-	-	*Chem. Sci.* **2012**, *3*, 2515.
Co-MoS_3 film	7	-	87	-	-	-	*Chem. Sci.* **2012**, *3*, 2515.
Ni-MoS_3 film	7	-	96	-	-	-	*Chem. Sci.* **2012**, *3*, 2515.
Cu-MoS_4 crystals	7	160	95	2	210	~100%	*Energy Environ. Sci.* **2012**, *5*, 8912.
MoS_3 film	7		86	-	-	-	*Chem. Sci.* **2012**, *3*, 2515.
Co-NRCNTs	7			2	380	-	*Angew. Chem. Int. Ed.* **2014**, *53*, 4372.
Mo_2C	7	-	-	1	200	-	*Angew. Chem. Int. Ed.* **2012**, *51*, 12703.
Mo_2B	7	-	-	1	250	-	*Angew. Chem. Int. Ed.* **2012**, *51*, 12703.

Table S3. Comparison of various solid-state HER catalysts in basic solutions.

catalyst	pH	Onset η(mV)	Tafel slope (mV/dec)	Current density (j, mA/cm^2)	η at the corresponding j (mV)	Faraday efficiency	Ref
Ni_2P - G@NF	14	~7	30	10	50	~100%	This work
CoP/CC	14	80	129	10	209	~100%	*J. Am. Chem. Soc.* **2014**, *136*, 7587.
Ni-Co sulphide	14	-	81	-	-	-	*Int. J. Hydrogen Energy* **1991**, *16*, 1.
CoS/FTO	14	100	-	1	480	-	*J. Am. Chem. Soc.* **2013**, *135*, 17699.
MoB	14	140	59	-	-	-	*Chem. Sci.* **2012**, *3*, 2515.
Ni	14	-	-	10	400	-	*Angew. Chem. Int. Ed.* **2012**, *51*, 12703.
Ni wire	14	~190	96	10	350	-	*ACS Catal.* **2013**, *3*, 166.
Co-NRCNTs	14	50-100	-	10	370	~100%	*Angew. Chem. Int. Ed.* **2012**, *51*, 12703.